2-D Magnetic Recording: Read Channel Modeling and Detection

Article *in* IEEE Transactions on Magnetics · November 2009

DOI: 10.1109/TMAG.2009.2023233 · Source: IEEE Xplore

CITATIONS
64

READS
1,032

6 authors, including:

Anantha Raman Krishnan
The University of Arizona
19 PUBLICATIONS **317** CITATIONS

SEE PROFILE

M. Fatih Erden
Seagate Technology
69 PUBLICATIONS **2,401** CITATIONS

SEE PROFILE

2-D Magnetic Recording: Read Channel Modeling and Detection

Anantha Raman Krishnan[1], Rathnakumar Radhakrishnan[1], Bane Vasic[1], Aleksander Kavcic[2], William Ryan[1], and Fatih Erden[3]

[1]Department of Electrical and Computer Engineering, Tucson, AZ 85721 USA
[2]Department of Electrical Engineering, University of Hawaii, Honolulu, HI 96822 USA
[3]Channels Department, Seagate Technology, Bloomington, MN 55435 USA

Two-dimensional magnetic recording (TDMR) is a novel storage architecture that, in theory, can achieve a density of up to 10 $\mathrm{Tb/in^2}$. It uniquely differs from other proposed next-generation architectures because of its reliance on sophisticated 2-D signal-processing algorithms. Recently, a number of contributions have been made in the development of read-channel models and detectors for TDMR systems. In this paper, we provide a detailed review on all important read-channel models under consideration. Our discussion focuses on the purpose of each model, placing a special emphasis on the suitability of the Voronoi model for the purpose of designing detectors. We also propose several detection schemes for TDMR based on the Voronoi model and present some numerical results.

***Index Terms*—Detectors, modeling.**

I. Introduction

In the last few years, many novel architectures have been proposed to increase storage densities of magnetic recording systems to 1 $\mathrm{Tb/in^2}$ and beyond. Two-dimensional magnetic recording (TDMR) [1] is the most recent among these architectures, which also includes heat-assisted magnetic recording (HAMR) [2] and bit-patterned media (BPM) [3]. Each of these are at different stages of development and pose various unique challenges. HAMR relies primarily on a novel read/write-head mechanism and BPM relies primarily on novel methods for producing ordered media for achieving high storage densities. Although an important component, signal-processing algorithms may not be a deciding factor in determining the feasibility of these systems. On the other hand, TDMR is uniquely different because it relies more on novel signal-processing algorithms, including detection and decoding.

TDMR attempts to store one bit in very few grains of the magnetic medium with an ultimate goal of storing 1 b/grain. It is interesting to note that under the assumptions of ideal write and readback, TDMR achieves the highest possible storage density for a given medium, unless some nonbinary magnetic storage techniques are developed in the future. However, formidable challenges need to be addressed before some conclusions on achievable densities can be derived. They arise as a consequence of the fact that the area of a bit in a TDMR system is comparable to the grain area. Since conventional media are used to store information in TDMR, the grain boundaries are irregular and form the primary source of noise. In addition to irregular boundaries, the random distribution of grains in the medium, along with the high areal density, necessitates the need for the information storage process to be viewed as a 2-D system. Therefore, there is a need for developing 2-D signal-processing algorithms and 2-D detectors and codes/decoders. Among the many challenges, the foremost is the development of a channel model for the purpose of designing these signal-processing algorithms.

In this paper, we discuss a number of TDMR channel models that are being studied. We explain the purpose for which each of these models was developed and emphasize the relationship between them. Further, we discuss some detector architectures for some of these channel models that provide a framework for evaluating uncoded and coded error-rate performance of TDMR systems at various storage densities. Throughout this paper, we point out the challenges that need to be overcome and provide some quantitative results where available. Overall, the goal of this paper is three fold: 1) to provide a survey of existing channel models for TDMR; 2) to explain the technical and methodological issues in developing 2-D signal-processing algorithms; and 3) to present some detector architectures, report on their performance, and provide some directions for future research.

The rest of this paper is organized as follows: Section II gives an overview of different models that are being considered for characterizing the TDMR channel. Section III illustrates the relationship between these models. Some detection strategies designed for the TDMR channel, along with some preliminary results are shown in Section IV. Finally, we summarize our work in Section V.

II. Read-Channel Models

Developing a channel model for TDMR mainly consists of three components: 1) a method for generating the recording medium; 2) modeling the data writing process; and 3) modeling the readback process. Each of these can be developed with varying degrees of complexity and accuracy. Since TDMR was first proposed, three different models have received much attention in the context of determining achievable areal densities in TDMR from a signal-processing perspective. These are the Voronoi model, discrete-grain model, and error-erasure model. We will discuss each model in some detail.

A. Voronoi Model

Before we describe the model for the recording medium, for the sake of completeness, we give a brief introduction to the Voronoi tiling of planes. Let $\mathcal{S}$ be a set of points on the Euclidean plane. Then, the Voronoi region of the point $s \in \mathcal{S}$, $\mathcal{A}_s$ is the

Manuscript received March 14, 2009; revised April 17, 2009. Current version published September 18, 2009. Corresponding author: B. Vasic (e-mail: vasic@ece.arizona.edu).

Digital Object Identifier 10.1109/TMAG.2009.2023233

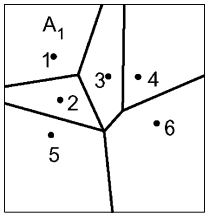

Fig. 1. Voronoi tiling of a plane.

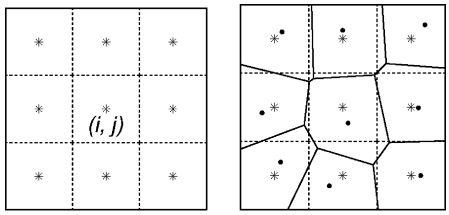

Fig. 2. Modeling of the recording medium. (a) Example of an ideal medium. (b) Example of a nonideal medium.

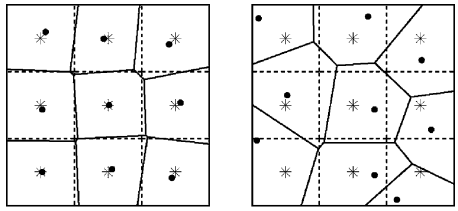

Fig. 3. Distribution of the shift of grain centers. (a) An example of a distribution with small average shift. (b) Example of a distribution with large average shift.

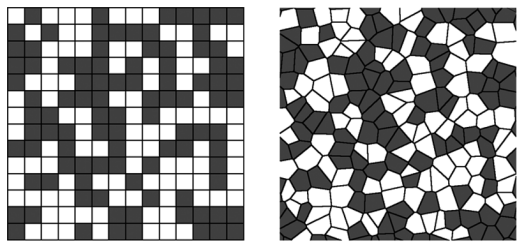

Fig. 4. Write model for the Voronoi medium. (a) Magnetization of an ideal medium. (b) Magnetization of a nonideal medium.

set of all points in the plane closer to s than to any other point belonging to $\mathcal{S}$. Fig. 1 shows an example of Voronoi tiling. The figure shows the regions of points 1 through 6. For example, the region $\mathcal{A}_1$ contains the points which are closer to 1 than to points 2–6. All of the points on the boundary are equidistant from their two closest points.

We seek to model the recording medium as a Voronoi tiling of a plane with every Voronoi region representing a grain. There is more than one way to produce a random Voronoi tiling of a plane. A natural approach is to first place some number of points randomly on a plane and construct their corresponding Voronoi regions. This would represent a recording medium with as many grains as the number of points in the set. One undesirable consequence of this approach is the large variance in grain size in the recording medium. However, this can easily be overcome by some simple techniques [1], [4] (e.g., by dividing large grains and combining small grains). Though a simple approach, this method gives a realistic representation of the recording media with very low correlation in the grain shapes and positions. However, it poses some difficulty in analyzing characteristics of noise that arise from irregular grain boundaries. Therefore, we develop another approach that allows us to define and analyze noise characteristics, at the same time preserving the random distribution of grains.

In our model, all instances of recording medium are assumed to be produced by a perturbation of the "ideal" medium (from the perspective of the detector). The ideal medium is one in which all grains would be of equal size and would be regularly spaced, and it can be visualized as the Voronoi tiling of points on a square lattice.

Let S be a set of points on the square lattice. Then, the Voronoi regions of points belonging to S correspond to the grains in the ideal medium. We refer to the points in S as cell centers and to their regions as cells. Fig. 2(a) shows an example of a plane of dimension 3×3 cells with the cell centers marked as "$*$." The cell boundaries are marked by dashed lines.

The randomness in the shape and position of grains is modeled by shifting the grain centers randomly from the cell centers. The recording medium can then be visualized as the Voronoi tiling of the shifted grain centers with their regions representing the grains. Fig. 2(b) shows an instance of recording medium of size 3×3 cells. The cell centers are marked as "$*$" and the shifted grain centers are marked as "$\bullet$." The cell boundaries are marked by dashed lines and the grain boundaries are marked by solid lines.

In modeling the medium this way, we assume that the shift of grain centers from their ideal positions follows some known probability distribution and that the shifted grain centers are always within their corresponding cells. Note that the choice of the distribution affects the degree of variation in the grain sizes, positions, and their boundaries. Fig. 3 illustrates the effect of choice of distribution on these parameters with two examples. The medium shown in Fig. 3(a) has a smaller average shift in grain centers than the one shown in Fig. 3(b). The boundaries of the ideal medium are denoted by the dotted line. It is readily seen that the medium shown in Fig. Fig. 3(a) is "closer" to the ideal medium than the medium shown in Fig. 3(b). Without prior knowledge, it is reasonable to assume that the shifts are uniformly distributed within the area of the cell. Admittedly, the choice of uniform distribution introduces long-term correlation in grain shapes and positions. Generalizations of this model are possible by using distributions which allow the grain centers to cross their corresponding bit boundaries (e.g., the Gaussian distribution).

The read/write mechanism of the TDMR system does not have any *a priori* knowledge of the grain shapes and sizes in the medium. Therefore, the write head simply assumes that the medium is ideal and attempts to write at the center of each cell. The grain, whose center is within the cell, is then appropriately magnetized. An example of the difference between the magnetization of an ideal medium and an actual medium as a result of this writing process is shown in Fig. 4. Fig. 4(a) and (b) shows the magnetization of an ideal and the actual 14×14 medium, respectively. The grains with magnetization $+1$ are colored black

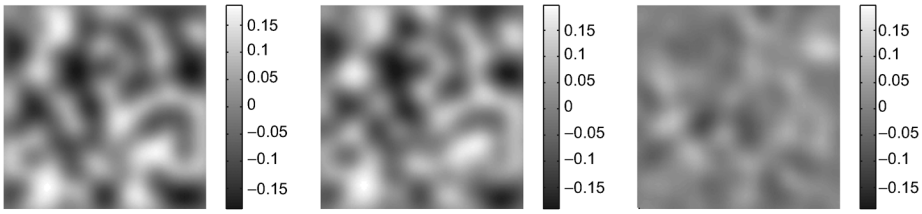

Fig. 5. Noise in TDMR. (a) Readback signal corresponding to Fig. 4(a). (b) Readback signal corresponding to Fig. 4(b). (c) Difference between the two readback outputs.

and the ones with magnetization -1 are colored white. The readback signal is obtained by convolving the magnetization of the medium with the read-head response and then sampling at cell centers. The response of the read head can be obtained by using the method proposed in [5]. We assume the response to be a truncated 2-D Gaussian pulse of unit energy with a half maximum of 1-bit period and a span of three 3-bit periods in both dimensions.

Our Voronoi model captures the noise characteristics generally observed in TDMR. With this model, it is feasible to study these characteristics, which aids in the design of detectors. Below, we discuss some of the important observations made by using this model.

1) Write Errors: The write model described before is a simplistic model that ensures that every bit is written to a unique grain, thereby avoiding any loss of information due to overwrite. It offers some computational advantages when implemented in software. In real-world systems, there may be write errors. To incorporate this into the channel model, a write model can be envisioned in which some grains are overwritten and some bits are not written into the recording medium at all. For instance, whenever the head tries to write at the center of a cell, we can assume that it magnetizes the grain that contains the center of the cell, rather than the grain whose center is contained in the cell. Such a model would introduce overwrite errors. Another way to naturally incorporate write errors into the channel model is by choosing the grain centers completely randomly while modeling the recording medium (of course, some means to reduce the grain variance should be incorporated when modeling the channel this way).

We observe that in the presence of write errors, bits lost to write errors can never be recovered by any detector. We can only hope to recover such information by the use of error-correcting codes. Therefore, it is reasonable to assume that these errors will not play a big role in designing detectors.

2) Noise Coloration: Viewing an instance of the recording medium as a deviation from the ideal medium allows us to define noise in the TDMR system in a natural way. In an ideal medium, as a result of the 2-D nature of the read-head response, the readback signal at the center of any cell (i,j) depends on the polarity of the grains in its $3\times$ 3 neighborhood, $\mathcal{N}_{i,j}$ [as depicted in Fig. 2(a)]. However, in practice, there is a change in the readback signal due to the shift in the grain boundaries. This change in the output is considered as noise. For example, Fig. 5 shows the readback signal corresponding to the ideal and an instance of a nonideal-magnetized medium shown in Fig. 4. The difference between these two outputs is considered as noise and is shown in Fig. 5(c). The correlated nature of noise in the downtrack and crosstrack direction is clearly seen in the figure. The noise in the (i,j)th cell depends on the boundaries of grain in $\mathcal{N}_{i,j}$ as well as their polarities.

3) Data-Location Dependence: Although the primary source of noise in TDMR is due to the irregular grain boundaries, it is important to note that a boundary affects the output only if the two grains sharing it are of opposite polarity. Consequently, the irregular grain boundaries do not induce any noise if the input is all zero or all one (when all of the grains are magnetized to the same polarity). In general, the consequence of this property is that the noise in a cell (i,j) depends not only on its neighborhood $\mathcal{N}_{i,j}$, but also on the location of transitions in its neighborhood.

Consider the (i,j)th cell in an ideal medium. It shares an edge with four cells (edge-sharing neighbors) and a vertex with four other cells (vertex-sharing neighbors). The (i,j)th cell, along with these eight cells, forms its neighborhood $\mathcal{N}_{i,j}$. The output of the (i,j)th cell $y_{i,j}$ depends not only on the polarity of the (i,j)th cell, but also on 1) the number of edge-sharing neighbors with polarity $+1$ and 2) the number of vertex-sharing neighbors with polarity $+1$. The symmetry in the read-head response ensures that the contribution of an edge(vertex)-sharing neighbor to the output $y_{i,j}$ is independent of its position relative to the (i,j)th cell. As an example, consider the output at the center of two 3×3 inputs (read row-wise) $[(-1+1-1),(-1-1+1),(-1-1-1)]$ and $[(+1-1+1),(-1-1-1),(-1-1-1)]$. The inputs are shown in Fig. 6(a) and (b), respectively. The outputs corresponding to Fig. 6(a) and (b) are equal because they have the same polarity in the center cell and have an equal number of edge- and vertex-sharing neighbors with polarity $+1$. Similarly, the outputs corresponding to Fig. 6(c) and (d) are equal. We say that all 3×3 neighborhoods with the same polarity of the center cell and the same number of edge-sharing and vertex-sharing neighbors with polarity $+1$ belong to the same configuration class. For a given instance of a nonideal recording medium, the output corresponding to each 3×3 input differs, even if they belong to the same configuration class, because of the asymmetric grain boundaries. However, since all instances of the recording medium are equally likely, their effect on the output will be the same statistically. This enables us to reduce the number of probability distribution functions required to characterize the noise, as will be seen in the next section.

4) Output Probability Density Function: In order for this model to be used in conjunction with a detector, it is important to determine the noise or output probability densities. If $\mathbf{X}=\{x_{1,1},x_{1,2},\ldots,x_{n,n}\}$ is a sequence of binary input to be stored in a medium of size $n\times n$ cells and $\mathbf{Y}=\{y_{1,1},y_{1,2},\ldots,y_{n,n}\}$ is the received signal at their corresponding cell centers, then

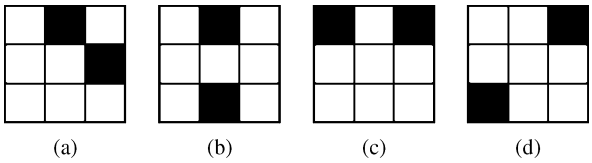

Fig. 6. Symmetry in the ideal medium. The final output at the center cell in Fig. 6(a) and (b) is equal. The output at the center cell in Fig. 6(c) and (d) is equal.

ideally, the characterization of noise in TDMR entails the estimation of the conditional probability density function (pdf) $p(\mathbf{Y}|\mathbf{X})$. However, the correlated nature of this noise makes it very difficult to estimate this quantity. The exact nature of correlation is difficult to estimate. As a simplification, we ignore the correlation and assume that the noise samples are independent of each other. We can then attempt to estimate $p(y_{i,j}|\mathbf{X})$. It is possible to estimate this quantity experimentally by means of histograms. The number of possible 3×3 binary inputs is $2^9 = 512$, which implies that 512 conditional pdfs are required. However, symmetry in the read-head response can be exploited to reduce the number of pdfs required to 25. Please refer to [6] for a detailed discussion. The pdfs obtained by this method reveal that there is a very high overlap among them, thereby indicating the challenge involved in reliable detection and decoding.

B. Discrete-Grain Model

Voronoi models, although accurate, are not well suited for the purpose of calculation of capacity of the TDMR channel. Hence, it is necessary that simpler models be developed, which makes the problem more tractable. The discrete-grain model is one such model that attempts to model the recording medium by representing its constituent grains as being one of a finite number of predefined shapes.

As in the case of the Voronoi model, the starting point of the discrete grain model is the ideal medium; the ideal medium is defined to be one in which all grains span 1 cell exactly. The variation in grain shapes and sizes can be modeled by letting the grains span over 1, 2, ..., or k adjacent cells with probability $p_1, p_2, \ldots, p_k$, respectively. Hence, the number of shapes that a grain can take is finite. Fig. 7 shows all possible shapes of grains spanning up to three adjacent cells. These collections of adjoining cells are called polyominoes or animals [7]. The recording medium can now be modeled as a tiling of a plane with a given set of polyominoes and with an appropriately chosen probability distribution.

This model can be simplified by restricting the possible shapes of grains. One such simplification is when the grain shapes are restricted to be rectangles of dimension $k_x \times k_y$, with probabilities p_{k_x,k_y}, where $1 \leq k_x \leq K_x$, $1 \leq k_y \leq K_y$ for appropriately chosen K_x, K_y. Fig. 8 shows the possible shapes of grains for $K_x = 2$ and $K_y = 2$.

Although the tiling of plane with dominoes (polyominoes spanning two cells) has been studied in the past [8], [9], the problem of tiling a plane with a set of polyominoes is, in general, a nontrivial problem (e.g., [7] and [10]). This, compounded with the fact that a probability distribution exists that governs the occurrence of polyomino, makes the problem even more difficult.

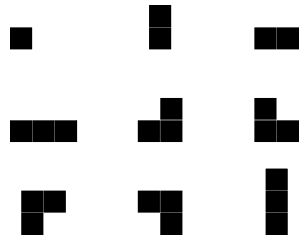

Fig. 7. Grains of size 1, 2, and 3.

Fig. 8. Possible shapes of grains for $K_x = 2$ and $K_y = 2$.

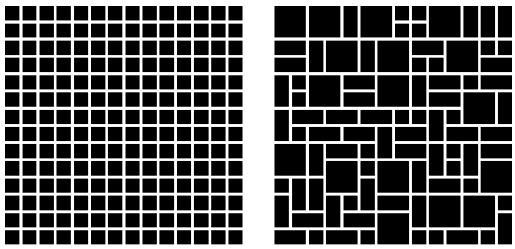

Fig. 9. Modeling of the discrete-grain medium. (a) Ideal medium. (b) Nonideal medium.

In practice, this is partly overcome by first partially covering the plane with the polyominoes drawn from the correct probability distribution until all of the uncovered portions of the plane are such that they cannot fit one or more of the possible polyominoes. Then, these "gaps" are filled with polyominoes chosen from a subset of the polyominoes which can fit in these areas. Note that this method of tiling changes the probability distribution of the polyominoes slightly. Fig. 9 shows an example of a medium created by using this method. Fig. 9(a) shows an ideal medium of size 14×14 and Fig. 9(b) shows an example of a medium consisting of grains of sizes up to 2×2 cells. For more details on this model and other discrete grain models derived from Voronoi models, readers are referred to [4].

The write process is modeled in a simple fashion. The write head writes at the centers of each cell in a row-by-row fashion and the grain which contains the cell is appropriately magnetized. Consequently, grains spanning one cell are magnetized exactly once and grains spanning more than one cell are written more than once. The final magnetization of the each grain is the magnetization that is written last onto one of its constituent cells. For instance, if the cell centers are written in a row-by-row fashion starting from the top-leftmost cell of the medium and ending in the bottom-rightmost cell, then the magnetization of each grain would be the magnetization of its bottom-rightmost constituent cell. As a result of overwrite, some of the input bits are irrecoverably lost [1]. Fig. 10(a) and (b) shows the magnetization of an ideal and nonideal medium resulting from such a write process. By inspecting the 2×2 grain at the top-leftmost position in Fig. 10(b), it can be seen that magnetization of the three of its constituent cells are overwritten. To model the read-back process, it is assumed that the resolution of the read head

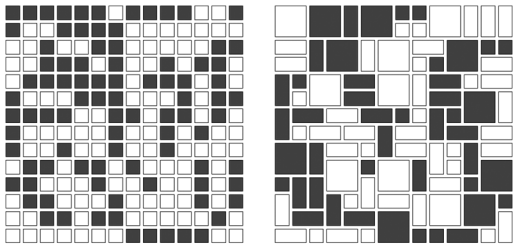

(a) (b)

Fig. 10. Write model for the discrete-grain medium. (a) Ideal medium. (b) Nonideal medium.

is high enough to read the magnetization of each cell without interference from adjoining cells.

As can be seen from the modeling of the write/readback process, all of the errors in this model occur during the write process. The capacity of this channel is defined as the average number of bits per grain that can be stored and retrieved without any errors. From this definition of capacity, it is evident the capacity of a recording medium with no variability in grain shapes is 1 b/grain. The capacity reduces when the grain shapes are variable. Some lower bounds on the capacity have been obtained for the 1-D equivalent of this channel $(K_x = 3, K_y = 1)$. The results indicate that the capacity is in the range of 0.6 to 1 b/grain [1].

C. Binary Error and Erasure Model

This model is the simplest among all of the models under consideration for the TDMR channel. It seeks to model the TDMR channel as a channel where bits are either: 1) erased with a probability ϵ (erasure probability); 2) transmitted incorrectly with a probability p (error probability); or 3) transmitted correctly (with a probability $(1-p-\epsilon)$. Hence, all errors in the recording process that occur due to the write/readback process are encapsulated within the model, obviating the need for a model of the recording medium. Although this model is not accurate, it is well suited for the design and evaluation of error-control codes and decoders for TDMR systems.

III. Relationship Between Various Models

The channel models discussed in the previous section can be considered to span a spectrum (Fig. 11), representing all possible models for TDMR. On one end of this spectrum is the micromagnetic model, which can accurately define each process involved in modeling the channel and is suitable for studying and optimizing various head/media dimensions and characteristics [4]. However, its high complexity renders it unsuitable for developing and studying various signal-processing algorithms. On the other end of the spectrum is the binary error-erasure model that represents the cascade of the write/read process and detection. Though it may be an oversimplification of the channel, it is suitable for an initial analysis of various codes and decoders. The model based on the Voronoi region achieves a good tradeoff between complexity and accuracy and, therefore, can be used for the purpose of designing detectors and evaluating codes/decoders [6]. The discrete-grain model may be relatively simpler, but is suitable for providing bounds on the capacity of the TDMR channel and will guide in determining the need for sophisticated detectors and decoders.

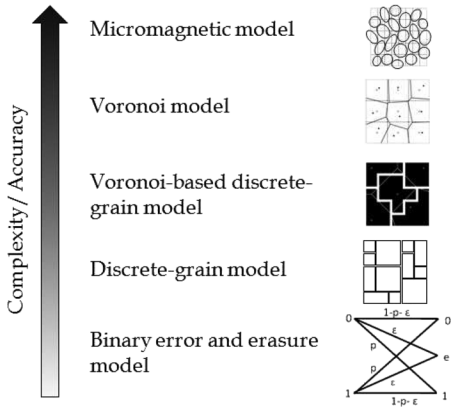

Fig. 11. TDMR read-channel model spectrum.

The discussion on Voronoi models and discrete-grain models in the previous section brings out many differences between them, particularly in the representation of the recording medium. However, it is possible to view both of these models in a unified way. In particular, some discrete-grain recording media can be considered to be coarsely quantized versions of the Voronoi tilings of the medium. Naturally, one could also consider a model for the recording medium with a finer quantization of the Voronoi region. We call this model the Voronoi-based discrete-grain model and was first suggested by Kheong *et al.* [4].

The relationship between the binary error-erasure model and the Voronoi model is more esoteric. To see this, first consider the equation for the readback signal in the ideal Voronoi medium. This can be written as

$$y_{i,j} = \sum_{(k,l)\in\mathcal{N}_{i,j}} x_{k,l} h_{i-k,j-l} \tag{1}$$

where $x_{k,l} \in \{-1, +1\}$ is the magnetization of the cell at the (k,l)th position and $h_{i-k,j-l}$ is the integral of the head response over the cell at the $(i-k, j-l)$th cell. From the discussion in Section II-A, it can be readily seen that $h_{a,b}$ is zero for (a,b) not in $\mathcal{N}_{i,j}$. To express (1) in words, the readback signal is the discrete convolution of the input magnetization with the discretized read-head response. That is

$$y_{i,j} = (x * h)_{i,j}. \tag{2}$$

Now, consider the readback signal of the nonideal Voronoi medium. Suppose, we were to model it similar to (1), then we would have

$$y_{i,j} = (\tilde{x} * h)_{i,j} \tag{3}$$

where $\tilde{x}_{i,j} \in \mathbb{R}$. The continuous nature of $\tilde{x}$ can be attributed to incursions into a cell from adjacent grains, which is a result of the irregularities in the grain boundaries. Equation (3) can also be interpreted as follows: if the detector is simply a zero-forcing equalizer which assumes the medium to always be ideal, then its output would precisely be $\tilde{x}_{i,j}$. That is

$$\tilde{x}_{i,j} = (h^{-1} * y)_{i,j}. \tag{4}$$

We refer to $\tilde{x}_{i,j}$ as the effective magnetization of the (i,j)th cell. The definition of effective magnetization can also lead to the in-

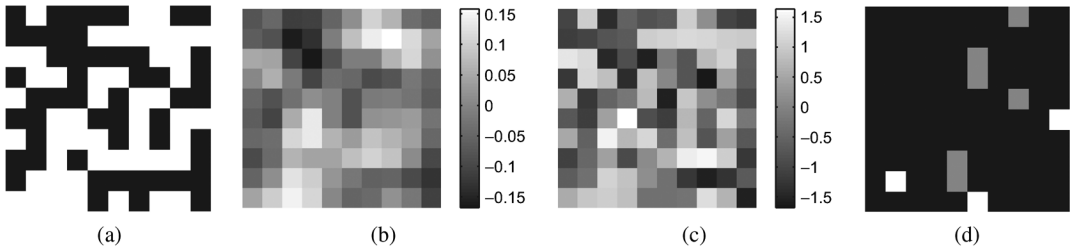

Fig. 12. Discrete convolution interpretation of the write/read process. (a) Bits written on a nonideal medium. (b) Sampled readback output. (c) The effective magnetization. (d) Error and erasures due to thresholding ($t = 0.2$).

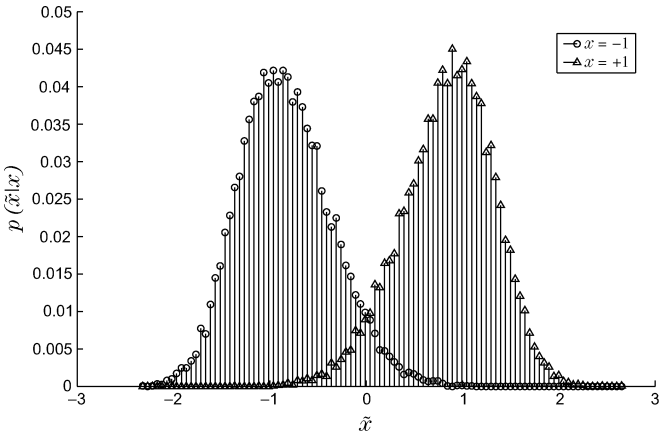

Fig. 13. Conditional pdf of the effective magnetization given with the input.

terpretation of the TDMR channel as a channel with response h with real inputs $\tilde{x}$. Fig. 12(a) shows the input magnetization written onto a nonideal medium. The sampled readback signal is shown in Fig. 12(b). The effective magnetization obtained at the detector is shown in Fig. 12(c). Fig. 13 shows the conditional probability density function $p(\tilde{x}_{i,j}|x_{i,j})$ that was obtained experimentally.

We can now establish a relationship between the two models. By selecting some threshold $t \geq 0$, we define

$$\hat{x}_{i,j} = \begin{cases} 1, & \text{if } \tilde{x}_{i,j} > t \\ -1, & \text{if } \tilde{x}_{i,j} < -t \\ \epsilon, & \text{if } -t \leq \tilde{x}_{i,j} \leq t. \end{cases} \quad . \tag{5}$$

For any t, we have a binary error erasure channel with the error and erasure probabilities given as

$$p = \int_{\tilde{x}>t} p(\tilde{x}|x=-1) + \int_{\tilde{x}<-t} p(\tilde{x}|x=1) \tag{6}$$

$$\epsilon = \int_{|\tilde{x}|\leq t} p(\tilde{x}|x=-1) + \int_{|\tilde{x}|\leq t} p(\tilde{x}|x=+1). \tag{7}$$

For a threshold $t = 0.2$, the errors and erasures corresponding to the effective magnetization in Fig. 12(c) are shown in Fig. 12. In the figure, errors are denoted by white-colored cells and erasures are denoted by gray-colored cells. The threshold can be chosen so that it maximizes the capacity of its corresponding binary error and erasure channel.

IV. Detection Strategies

Detection for the TDMR channel differs from detection for conventional channels because the primary source of noise in TDMR is the presence of the highly irregular bit/grain boundaries. Design of a detector which accounts for the high 2-D correlation of the noise is a considerable challenge. However, by assuming that the noise samples are independent of each other, it is possible to design schemes that detect user bits in the presence of 2-D ISI. In particular, the use of maximum-likelihood (ML) and maximum *a posteriori* (MAP) detectors that operate on the trellis or graph of the TDMR channel is possible.

A. Trellis-Based Detection

For the use of ML detectors, we can treat the TDMR channel as a multitrack model [11], where each row is considered to be a track. The three-track Viterbi algorithm (3TVA) [12] and decision feedback Viterbi algorithm (DFVA) [13] are two well-known multitrack detectors.

Let $\mathbf{X}$ and $\mathbf{Y}$ be the input bits and the sampled readback output. If X_i and Y_i are the input bits and the sampled readback output of the i^{th} track, respectively, then the three-track Viterbi algorithm operating on the ith track attempts to compute

$$\arg \max_{X_{i-1},X_i,X_{i+1}} P(Y_i|X_{i-1}, X_i, X_{i+1}) \, \forall i. \tag{8}$$

3TVA operates independently on each track in parallel. For every track i, the decision made on X_{i-1} and X_{i+1} are discarded. DFVA is similar to 3TVA but operates sequentially on a track-by-track basis. For every track i, the decision made on X_i is used as side information for the subsequent operation of DFVA on track $i+1$.

B. Detection Based on Probabilistic Graphical Models

The optimal MAP detector calculates for each $x_{i,j}$, the *a posteriori* probability $P(x_{i,j}|\mathbf{Y})$. The calculation of this probability is nontrivial. However, this can be calculated approximately by using the sum-product algorithm (SPA) [14]. Let $\theta_{i,j}$ be a 9-tuple denoting the value of the 3×3 neighborhood of $x_{i,j}$. Let θ^0 (θ^1) be the set of values of $\theta_{i,j}$ for which $x_{i,j} = 0$ (1). If for every i, j, suppose the *a posteriori* probability $P(\theta_{i,j}|\mathbf{Y})$ can be calculated, then the MAP estimate $x_{i,j}$ can be determined as

$$\hat{x}_{i,j} = \begin{cases} 0, & \text{if } P^0_{i,j} > P^1_{i,j} \\ 1, & \text{else} \end{cases} \tag{9}$$

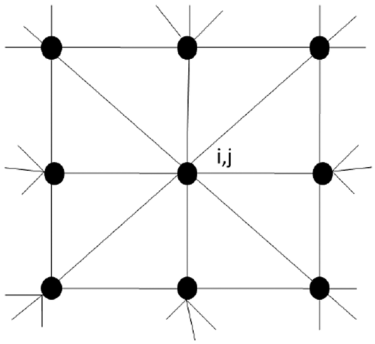

Fig. 14. Graph representing the TDMR channel.

where

$$P^0_{i,j} = \sum_{\theta_{i,j} \in \theta^0} P(\theta_{i,j}|\mathbf{Y}) \tag{10}$$

$$P^1_{i,j} = \sum_{\theta_{i,j} \in \theta^1} P(\theta_{i,j}|\mathbf{Y}). \tag{11}$$

In order to calculate the probability $P(\theta_{i,j}|\mathbf{Y})$, we first define a graph that represents the TDMR channel and then operates SPA on it. In this graph, each node (i,j) represents the local neighborhood $\theta_{i,j}$. The graph is shown in Fig. 14. The message from any node (say (i,j)) in this graph to its neighboring node (say (i_1,j_1)), $m_{(i,j)\to(i_1,j_1)}$ can be given as

$$m_{(i,j)\to(i_1,j_1)} = \sum_{\theta_{i,j}} P(y_{i,j}|\theta_{i,j}) P(\theta_{i,j}|\theta_{i_1,j_1}) \cdot \prod_{(i_2,j_2)\in \mathrm{N}_{i,j}\setminus\{(i_1,j_1)\}} m_{(i_2,j_2)\to(i,j)}. \tag{12}$$

The probability $P(\theta_{i,j}|\mathbf{Y})$ is given as

$$P(\theta_{i,j}|\mathbf{Y}) \approx P(\theta_{i,j}) P(y_{i,j}|\theta_{i,j}) \prod_{(i_1,j_1)\in N_{i,j}} m_{(i_1,j_1)\to(i,j)}.$$

The approximation is due to the presence of cycles in the factor graph. Better approximations of *a posteriori* probabilities may be possible with the use of generalized belief propagation algorithms [15], [16].

C. Simulation Results

For the simple detector which simply decides on the bit based on its polarity, the bit-error rate (BER) is 31%. For the detectors described before, the BERs are in the range of 13%–16%. The high BER obtained by these detection schemes is a consequence of the assumption that the noise samples are independent and the large overlap among the output conditional pdfs.

In order to reduce the bit-error rate, we need to look at more sophisticated detection schemes which consider the correlation between noise samples. Another approach can be the use of constrained codes which attempt to reduce the overlap between conditional pdfs. However, this comes with the penalty of reduced recording rates.

V. Summary

In this paper, we have provided an overview of all the channel models pertinent to signal processing in TDMR. Varying in accuracy and complexity, these models provide groundwork for addressing some of the challenges present in this technology, such as estimation of capacity of the TDMR channel, design of detectors, and design of codes and decoders for this channel. Also, we establish a relationship between the binary error and erasure model and the Voronoi model that unifies these two seemingly disparate channel models. Finally, we have also outlined some detector architectures for the TDMR channel. The preliminary results indicate the need for more sophisticated detectors which account for the correlation between noise samples.

Acknowledgment

This work was supported in part by INSIC-EHDR and in part by the National Science Foundation under Grants IHSC-0725405 and CCF-0634969.

References

[1] R. Wood, M. Williams, A. Kavcic, and J. Miles, "The feasibility of magnetic recording at 10 terabits per square inch on conventional media," *IEEE Trans. Magn.*, vol. 45, no. 2, pt. 2, pp. 917–923, Feb. 2009.

[2] R. E. Rottmayer *et al.*, "Heat-assisted magnetic recording," *IEEE Trans. Magn.*, vol. 42, no. 10, pp. 2417–2421, Oct. 2006.

[3] B. Terris, T. Thomson, and G. Hu, "Patterned media for future magnetic data storage," *Microsyst. Technol.*, vol. 13, no. 2, pp. 189–196, Nov. 2006.

[4] S. C. Kheong *et al.*, "TDMR platform simulations and experiments," *IEEE Trans. Magn.*, 2009, submitted for publication.

[5] D. T. Wilton, D.Mc.A. McKirdy, H. A. Shute, J. J. Miles, and D. J. Mapps, "Approximate three-dimensional head fields for perpendicular magnetic recording," *IEEE Trans. Magn.*, vol. 40, no. 1, pp. 148–156, Jan. 2004.

[6] A. R. Krishnan, R. Radhakrishnan, and B. Vasic, "Read-channel modeling for detector design of two-dimensional magnetic recording systems," *IEEE Trans. Magn.*, submitted for publication.

[7] S. W. Golomb, "Tiling with sets of polyominoes," *J. Combin. Theory*, vol. 9, pp. 60–71, 1970.

[8] Kasetelyn, "Statistics of dimers on a lattice," *Physica*, vol. 27, no. 12, pp. 1209–1225, 1961.

[9] N. Elkies, G. Kuperberg, M. Larsen, and J. Propp, "Alternating-sign matrices and domino tilings (part i)," *J. Algebraic Comb.*, vol. 1, no. 2, pp. 111–132, 1992.

[10] J. H. Conway and J. C. Lagarias, "Tiling with polyominoes and combinatorial group theory," *J. Comb. Theory Ser. A*, vol. 53, no. 2, pp. 183–208, 1990.

[11] S. Gopalaswamy and B. V. K. V. Kumar, "Multi-channel readback model for an optical tape system," in *Proc. Globecom*, 1994, pp. 1472–1476.

[12] B. G. Roh, S. U. Lee, J. Moon, and Y. Chen, "Single-head/single-track detection in interfering tracks," *IEEE Trans. Magn.*, vol. 38, no. 4, pp. 1830–1838, Jul. 2002.

[13] J. F. Heanue, K. Gurkan, and L. Hesselink, "Signal detection for pageaccess optical memories with intersymbol interference," *Appl. Opt.*, vol. 35, no. 14, May 1996.

[14] F. R. Kschischang, B. J. Frey, and H.-A. Loeliger, "Factor graphs and the sum-product algorithm," *IEEE Trans. Inf. Theory*, vol. 47, no. 2, pp. 498–519, Feb. 2001.

[15] J. S. Yedidia, W. Freeman, and Y. Weiss, "Constructing free-energy approximations and generalized belief propagation algorithms," *IEEE Trans. Inf. Theory*, vol. 51, no. 7, pp. 2282–2312, Jul. 2005.

[16] O. Shental, J. S. Yedidia, W. T. Freeman, and Y. Weiss, "Constructing free-energy approximations and generalized belief propagation algorithms," *IEEE Trans. Inf. Theory*, vol. 51, no. 7, pp. 2282–2312, Jul. 2005.